Soft Matter

PAPER

View Article Online
View Journal | View Issue

Cite this: *Soft Matter*, 2022, **18**, 2060

Microalgae *Chlorella vulgaris* and kraft lignin stabilized cellulosic wet foams for camouflage†

Nina Forsman,[a] Tia Lohtander,[a] Juha Jordan,[b] Ngoc Huynh,[a] Ari Seppälä,[c] Päivi Laaksonen,*[b] Sami Franssila[d] and Monika Österberg*[a]

Received 3rd December 2021,
Accepted 29th January 2022

DOI: 10.1039/d1sm01719e

rsc.li/soft-matter-journal

Plants, animals, and humans use camouflage to blend in with their surroundings. The camouflage is achieved with different combinations of colors, patterns, and morphologies. In stealth applications, the simplest camouflage uses textiles colored similarly to the environment to create an illusion. However, often, visible light range camouflage is not enough since the multispectral detection technologies of today are readily utilized for identification. Foams can be created with a straightforward fabricating process, and lightweight material exhibits good thermal insulation properties, providing stealth in the infrared light region. Herein, we produce cellulosic wet foams from surfactant and bleached pulp or cellulose nanofibrils. The visible light camouflage is created with green microalgae, *Chlorella vulgaris*, and brown kraft lignin, which also stabilized the foams. The thermal and spectral camouflage performance of foams was influenced by the cellulose content as well as the stability and water content of foams. Overall, these results give insight into how stability impacts the thermal and spectral properties of wet foams and provide a solid base for further material development to improve camouflage performance. While there is plenty of data on dry foams, the functional behavior of wet foams is currently not well known. Our method, using plant-based components can be exploited in a variety of other applications where simplicity and scalability are important.

1. Introduction

Animals and plants use camouflage to stay safe from predators by utilizing colors, patterns, and morphological structures to blend into the environment.[1] Nature's clever protection mechanism has also been adapted to human action. The most prominent example is military equipment, although nature photographers and guides frequently use camouflage materials as well. Similar to wildlife, the most basic human camouflage is patterned clothing designed to match natural surroundings, mostly green and brown shades in boreal forests and yellow and brown shades for sand lands. New coloring techniques are being developed all the time, including electrochromics[2,3] and adaptive materials.[4] Other camouflage techniques include structured textiles of metal incorporated yarn[5] and synthetic biology for advanced camouflage and protection materials.[6]

Military equipment for detection and identification are evolving, and due to widely utilized multi- and hyperspectral cameras capturing broader spectral ranges than simply the visual range,[7] camouflage materials nowadays need to be undetectable in greater spectral ranges than simply the visual range. Humans emit thermal radiation, and to conceal human activity, the infrared range needs to match the surroundings. Hence insulating materials – those with low thermal conductivity – need to be used. Due to the low thermal conductivity of air and their high air content, different kinds of foams, like polyurethane foams[8,9] are commonly used as insulators. Nanocellulose is a particularly interesting material for insulating foams due to the formation of extensive networks with plenty of voids in between, *i.e.*, porous systems.[10,11] Composite foams, such as polyurethane foams with cellulose nanocrystals,[12,13] is a way to tune the properties even further.

A simple way to produce an insulator is to use foam, *i.e.*, a colloid of gas bubbles dispersed in liquid or solid. A foam can be generated by mixing air and water or by leading gas through the water. Often a surfactant is needed to stabilize the foam; dispersed lignin can act as a surfactant.[14] Compared to stabilizing an emulsion, stabilizing a foam is more difficult due to the higher surface tension at the air/water interface than at the oil/water

[a] *Department of Bioproducts and Biosystems, School of Chemical Engineering, Aalto University, Espoo, Finland. E-mail: monika.osterberg@aalto.fi*
[b] *HAMK Tech, Häme University of Applied Sciences, Hämeenlinna, Finland. E-mail: paivi.laaksonen@hamk.fi*
[c] *Department of Mechanical Engineering, School of Engineering, Aalto University, Espoo, Finland*
[d] *Department of Chemistry and Materials Science, School of Chemical Engineering, Aalto University, Espoo, Finland*

† Electronic supplementary information (ESI) available. See DOI: 10.1039/d1sm01719e

interface, the larger density difference between a gas and a liquid than between two liquids, as well as the higher solubility and diffusivity of a gas in water than of typical oils in water.[15] Over time, the water drains from the foam phase, enabling the bubbles to coarsen and transfer gas from smaller to larger bubbles. To counteract these effects, a few measures can be taken. First, cellulosic fibers can be used to stabilize the bulk phase while surfactants decrease the surface tension at the interface.[16,17] Second, modifying the viscosity, either of the bulk liquid or by adding particles[18,19] or cellulose nanofibers[20] that assemble at the interphase, increasing the viscosity locally,[21] and slowing down the drainage.

To address the UN's Sustainable Development Goals (SDG 12.5 especially) and reduce reliance on limited sources of fossil raw materials and their negative effects on the planet, we strive to use non-toxic biomaterials.[22] While many conventional foams are made of fossil raw materials, in this work we focus on foams made from plant-based materials. As already discussed, both cellulose and CNF can be used in foams providing structure and delaying gas transfer between bubbles. Carbon nanotubes (CNCs) can be used in a variety of foam applications.[23,24] To stabilize the air–water interface, starch, both in the form of nanoparticles[25] or as such reinforced with CNF,[26] can be used. Proteins can also act as stabilizers.[27,28] Lignin has been used in composite foams for insulating purposes with both fossil and bio-based raw materials, but the structural complexity of lignin hampers its use.[29,30] To provide the color needed for stealth, there are a plethora of natural dyes, however, many dyes suffer from poor stability, limiting their applicability.[31] In the boreal forest, the most important colors are green and brown. The typical brown color is found in the tree trunks that obtain their coloration from lignin. Lignin is a readily available side stream from pulp production and could thus be used as the brown colorant. Additionally, lignin has been shown to possess amphiphilic properties and could hence act as a surfactant.[32] The green color of leaves is attributed to the photosynthetic chlorophyll a and b pigments.[33] One advantage of using biocolorants is that colorants derived from natural sources are likely to have similar spectral properties as the surroundings in the boreal forest.

Herein we present lightweight cellulosic biocolored foams as camouflage materials. To generate our foam, we used sodium dodecyl sulfate (SDS) as a surfactant and bleached kraft pulp and cellulose nanofibrils (CNF) as stabilizers. Since foams including cellulose are whiteish or colorless depending on the size of the cellulose fibrils/fibers, biocolorants are needed to obtain more natural colors. Lignin and microalgae *Chlorella vulgaris* were used as biocolorants to obtain a brown and green shade, respectively. The use of bio-colorants in foams is scarce and it is not known how they affect the foam formation and stability of wet and dry foams. The aim of this study was to assess and optimize the foamability and foam stability of green foams and evaluate the spectral and thermal properties of the foams. The foams were not dried prior to use, and to the best of our knowledge, the functional properties of wet foams have not been studied and the knowledge about the subject is lacking.

2. Experimental

2.1 Materials

Never-dried bleached birch pulp with 12.35% dry weight was obtained from UPM, Finland, and used as such in the pulp foams. The fibers' width were in the range of μm.[34] Never-dried bleached kraft birch pulp, washed into sodium form according to the method by Swerin,[35] was used to prepare cellulose nanofibrils (CNFs) using a high-pressure microfluidizer (Model M-110Y, Microfluidics, USA). The CNF fluidization method has been described comprehensively by Farooq *et al.*[36] In short, the Na washed pulp was passed through a series of 400 and 200 μm chambers, after which it was passed six times through a series of 400 and 100 μm chambers at a pressure of 2000 bar. CNF prepared in previous works according to the same procedure has had a fibril width of 5–20 nm[37] and a ζ-potential of −3 mV at pH 8.[38] Sodium dodecyl sulfate (SDS) was purchased from Sigma-Aldrich and used without further purification. Purified BioPiva kraft lignin was obtained from UPM. A powder of microalgae

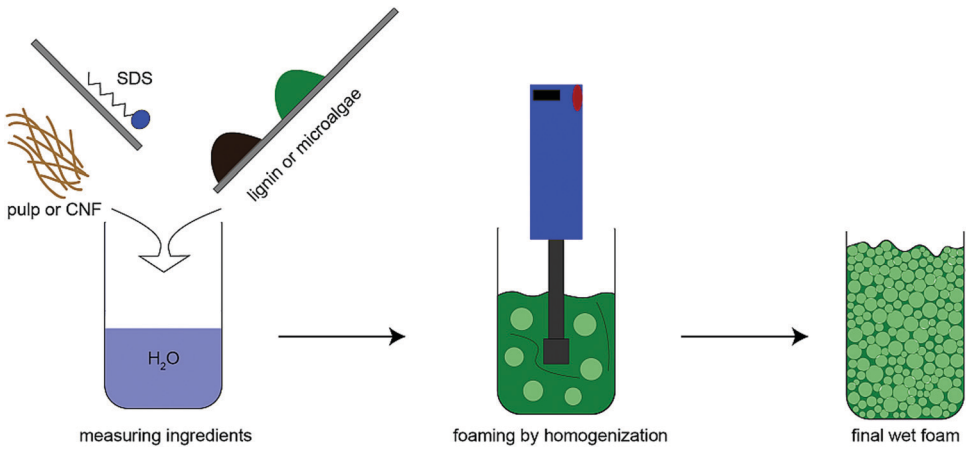

Fig. 1 Schematic illustration of the foaming process.

Chlorella vulgaris, intended for use as a dietary supplement, was purchased from a local organic food shop Ruohonjuuri. Deionized water was used in all sample preparations.

2.2 Preparation of foams

The schematic illustration of the foaming process is shown in Fig. 1. The desired amounts of bleached pulp or CNF, SDS, and microalgae or lignin were measured into a cup. Deionized water was added so that the total water volume was 12.5 mL. The water content in the pulp/CNF dispersion was taken into account. The mixture was then foamed using an Ultra-Turrax homogenizer (IKA T18, IKA Works GmbH & Co. KG, Germany) for 2 minutes at 1600 rpm. For the optimization experiments, the foam was immediately transferred into a measuring cylinder. This preparation method was used for all experiments except the thermal conductivity experiments, for which a slightly modified preparation method, described later, was used.

2.3 Modeling and optimization

The software Modde 8.0 (Umetrics, Sweden) was used for the foam composition optimization. Initial maximum and minimum concentrations for the different constituents were determined in previous experiments.[39] The same concentrations were used for microalgae as for lignin. A response surface model, based on the quadratic face-centered central composite (CCF) design, with three center points and two replicates, was used. Based on the maximum and minimum concentrations and the model, the software provided a test series, which were then carried out. In short, the minimum, average, and maximum concentrations of all three foam constituents were tested in 17 different combinations. The responses of the tests were initial foam volume and drainage after 5 minutes and 2 hours, all measured in milliliters (mL). In the software, the outliers were removed and the model was fitted, from which the response surfaces and optimal concentration ranges were obtained. For the optimization, the initial foam volume was maximized, whereas the drainage of the liquid volume was minimized.

2.4 Optical microscopy

The bubble size and microalgae properties were imaged with a Leica DM750 transmitted light microscopy. The right block of Fig. 4 and 5 were imaged with an Olympus BX53M with a DP74 camera with reflected and transmitted light and polarization.

2.5 Microalgae characterizations

The zeta-potential and size of the microalgae particles suspended in water were measured using a Malvern Zetasizer Nano ZS90. The chemical structure was measured using an attenuated total reflection Fourier-transform infrared (ATR FTIR) spectroscope (SpectrumTwo, PerkinElmer).

2.6 Viscosity measurements

Six samples were prepared according to the concentrations given in Table S2 (ESI†), and one extra sample was prepared by adding 132 g L^{-1} of microalgae into the 10.4 g L^{-1} of CNF to investigate the effect of chlorella on the viscosity of the CNF system. The samples were not foamed before the measurement. The viscosity measurements were performed at 23 °C with a controlled rate rheometer MCR 302 (Anton Paar) using a plain plate–plate geometry (diameter 25 mm). The apparent viscosity data was collected using rotational methods (shear rate range of 0.001–1000 s^{-1}) and the system was allowed to stabilize for 15 seconds before each measurement. Each sample was measured with three repetitions.

2.7 Thermal conductivity analysis

Thermal conductivity measurements were conducted with a CTherm TCi device exploiting a modified transient plane source technique. The device was calibrated with distilled water, LAF 6720 foam, and Pyrex. All chemicals were mixed with a homogenizer for 2 minutes to prepare ~270 ml wet foam samples. After the preparation, a 12 minute waiting period followed to allow most of the additional water to drain to the bottom of the container. Next, the measurement sensor was immersed approximately 2 cm deep in the sample. The sensor surface was oriented downwards to prevent water stratification on the sensor surface. Conductivity values were recorded for 2 hours. Additionally, we measured the change of height of foam layers as a function of time for analyses of the decay and the thermal resistance of the foam. The layer height was measured with a ruler. Three samples of each type of foam were prepared and tested.

2.8 Multispectral properties of wet foams

All foams and natural materials were photographed with a Specim IQ hyperspectral camera operating at wavelength range 400–1000 nm to examine spectral characteristics of the foams in comparison to natural materials.

3. Results and discussion

3.1 Optimization of microalgae foams

The goal of this work was to produce foams with appropriate camouflage characteristics. In other words, the requirements for the foams were sufficient foamability and stability, thermal insulation capability, and multispectral optical appearance similar to a boreal forest environment. Further in development, the system should be effortless to use in field conditions, and the components should be non-toxic and biodegradable in case the foams are not removed from nature. To achieve these characteristics, SDS, pulp/CNF, and dry microalgae *Chlorella vulgaris* in water was used. The optimization model was used to facilitate understanding of how the components influence the foam system and to obtain a recipe for an optimum foam in terms of maximum foamability and minimum drainage. The basis of the model was the minimum, medium, and maximum concentrations of each component, which were tested in a total of 17 different combinations according to the experimental matrix obtained from the software. The data gained was then fitted to the model, and response surface models, as well as an optimized foam formulation, was obtained. The foamability

and stability of lignin-containing CNF and bleached pulp foams were investigated earlier.[39]

3.2 Factors affecting foam stability

Almost any liquid can be temporarily foamed, but after a certain time, the foam begins to age through drainage of liquid from the foam phase and coalescence and coarsening of the bubbles. Investigating the stability of foams was essential for the application to maximize the durability of camouflage properties. The stability of foams was determined based on the drainage of the foams, measured as the amount of visible liquid under the foam (Fig. 2). The response surfaces of the drainage optimization showed that the most stable foams were achieved with high concentrations of pulp or CNF and microalgae. For all samples, the microalgae played an important role in the stability: the more microalgae added, the less drainage, and thus the better the stability of the foam. The effect of the microalgae was so significant that the drainage of the microalgae-containing foams was in some cases predicted to reach zero drainage, even after 2 hours (Fig. S1, ESI†). For the pulp samples, both higher SDS and pulp concentrations were contributing factors to counteract the drainage, even though the effect of the SDS concentration was stronger. The effect of cellulose concentration was also evident because more pulp or CNF led to lower drainage of the foam. CNF showed a better stabilizing effect than pulp since both the predicted minimum and maximum drainage for the CNF foams were lower than for the pulp foams. The main difference between pulp and CNF is the dimensions of the fibrils, which influence the surface area and rheology. The better stabilizing effect of CNF is probably due to the higher aspect ratio of CNF than of pulp, which allows nanosized fibers to form a tighter network around the bubbles. CNF also has a larger accessible area for stabilization, which also contributes to the cohesive interaction between the cellulose fibers themselves and increases the viscosity both at the interface and in bulk. The viscosity of foams is discussed later.

3.3 Factors affecting foaming

In addition to the stability of foams, the foamability of the system was considered to be a primary target since the do-more-with-less approach is desired in field conditions. The response surfaces of the foam volume optimization showed that increasing the SDS concentration led to larger volumes of initial foam for the pulp and CNF containing foams (Fig. 3). With both foam types, increasing the concentration of cellulosic material led to smaller foam volumes, although with pulp foams, the cellulose concentration range yielding maximum foam volume was wider than for CNF. Although the CNF is known to form more viscous gels than pulp, already at low concentrations, the maximum foam was generated within similar concentration ranges of SDS and either CNF or pulp. This is most likely due to the shear-thinning behavior of CNF,[40] meaning that the applied shear forces during the foaming reduce the viscosity of CNF allowing it to form a high volume of foam. Usually, increasing solids content and consequently increasing viscosity decreases the amount of trapped gas.[41] Interestingly, for CNF containing foams (Fig. 3 lower row), the foaming efficiency was slightly more dependent on the combinational concentrations of CNF and SDS rather than on CNF and SDS concentrations individually, as opposed to the pulp foams, although the difference was small. This difference can be

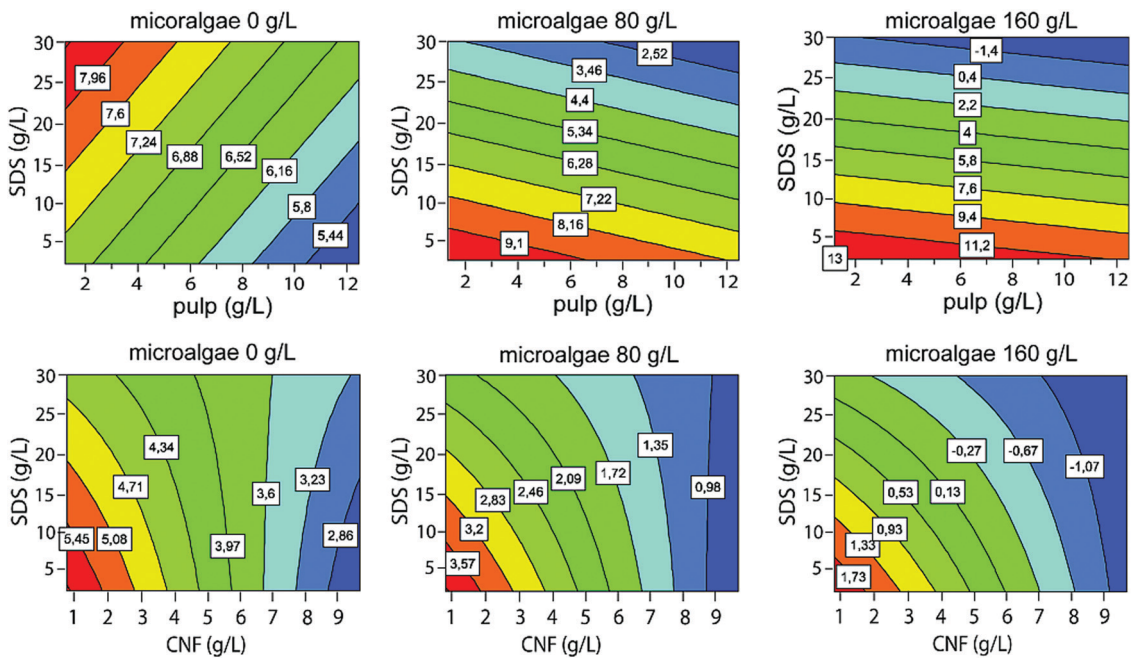

Fig. 2 The stability of foams containing bleached pulp (upper row) or cellulose nanofibrils (CNF) (lower row) with and without microalgae 5 minutes after foaming. The stability was investigated in terms of drained liquid (mL) using the response surfaces. The highest drainage volumes are marked with red and the lowest volumes with blue. The higher the microalgae content, the better the stability against drainage.

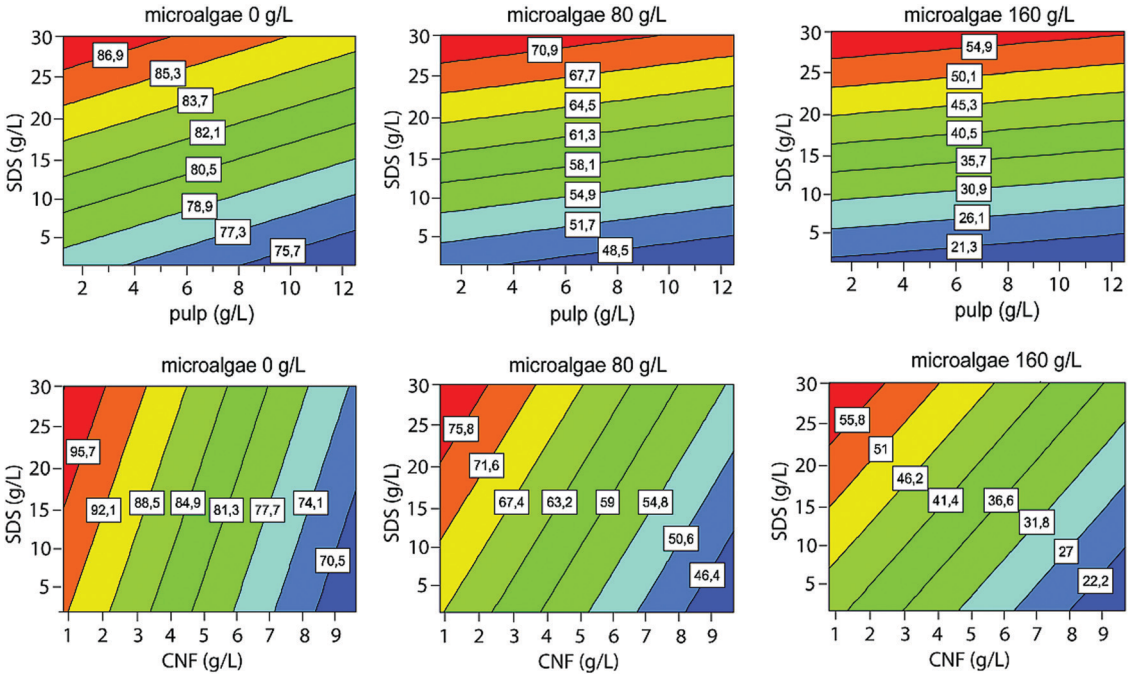

Fig. 3 The foamability of foams containing bleached pulp (upper row) or cellulose nanofibrils (CNF) (lower row) with and without microalgae. The foamability was investigated in terms of generated foam volume (mL) using the response surfaces. The highest foam volumes are marked with red and the lowest volumes with blue. The foams with high surfactant concentration, low cellulose, and microalgae concentrations led to the highest foam volumes with both pulp and CNF foams.

distinguished as a steeper slope for CNF foams in response surfaces (Fig. 3 lower row). This phenomenon was observed when a combination of high concentrations of pulp or CNF and microalgae were foamed where also the microalgae contributed to the viscosity increase. The response surface models for neat pulp and CNF foams differ slightly from our previous study,[39] which is most likely due to minor differences in the foaming process. The role of SDS in foaming is not surprising since SDS is a surfactant designed to stabilize the interface of a bi-phase system. Nanocellulose and pulp have to some extent been used to stabilize foams, although most often for the stabilization of dry foams.[11,18,42,43]

The most interesting observation was the significant effect of microalgae on the foaming of the system. Higher amounts of microalgae led to lower amounts of foam, regardless of applied cellulosic material. The trend was very clear for both pulp and CNF stabilized foams. Within this system, the maximum foam formation was obtained with a combination of low cellulose content and a high SDS concentration. It is possible that by going beyond the concentration limits used herein, the foam generation would have been even higher. These concentrations were initially optimized for systems with pulp/CNF, SDS, and lignin[39] and not for microalgae. The foaming was not either tested without SDS since the results shown here indicate the importance of surfactant for the foamability. From Fig. 1 it can be seen that the more microalgae added, the less foam was generated. Lignin did not improve foamability, which was addressed in our previous study.[39] A detailed description of the fitting and validity of models is presented in ESI,† (Tables S1–S3). The concentration limits of SDS were not increased due to economic reasons and to obtain comparable results. The microalgae consist of several chemical compounds, including lipids, and differs structurally from lignin and would thus require a slightly modified model. Even though the concentrations might not have been fully optimized for the microalgae foam, an understanding about the components' effect on the foaming process was still gained.

The effect of the microalgae was very interesting as it reduced the foamability, while it still significantly improved the foam stability over longer periods of time. It should still be kept in mind that the stability was only measured for 2 hours, which still is a relatively short period of time. However, the foams were placed in measuring cylinders and not spread over a surface as it is intended for the application. The geometry of the foam can influence its stability over longer periods of time. None of the studied foams were stable for several days but had drained almost completely (results not shown). Considering the intended application, the lack of long stability might not be a problem. For the intended use as a temporary camouflage material in the field, a few hours might be enough, and if longer coverage is needed, the foam can just be reapplied.

3.4 Bubble size and properties of microalgae *C. vulgaris*

The stability of foams investigated with response surface models showed the foams' ability to resist drainage. To evaluate the changes taking place in the foam phase during their aging, the optimized microalgae stabilized foams were imaged using a light microscope (Fig. 4). The lignin foams were evaluated in our previous study.[39] The bubbles of the foams made with

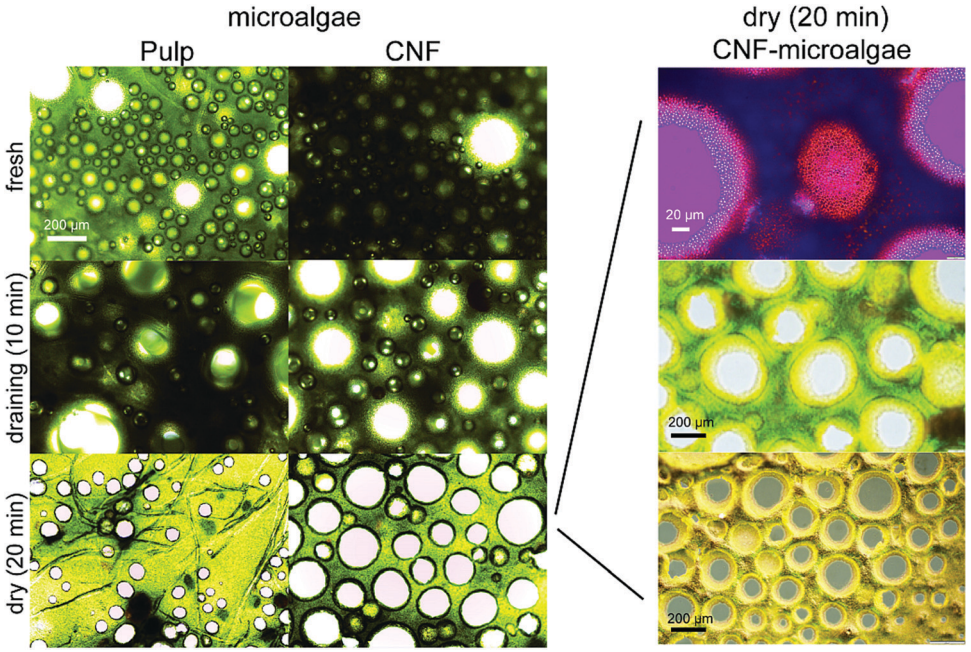

Fig. 4 Light microscopy images of the optimized pulp-microalgae and CNF-microalgae wet foams (left block). All images in the left block were taken at the same scale. Images were also taken with a microscopy with transmitted and reflected light and polarization (right block). A small amount of freshly generated foam was placed onto a glass slide, hence the foams have dried already after 20 minutes. The CNF-microalgae foam showed better stability than pulp-microalgae foam.

microalgae were generally in the range of 50–200 μm, but some bubbles fell outside this size distribution. Especially in the pulp foam, there was plenty of liquid between the bubbles. In the CNF foam, there seemed to be slightly less liquid between the bubbles, but the continuous phase was still clearly distinguishable. All bubbles were also round and not polyhedral. The liquid-filled space and spherical shape of bubbles indicate that both foams can be classified as wet foams.[44] Over time, there were some barely notable changes in the bubble size of the pulp foam due to coalescence and coarsening since the bubbles generally appeared to be slightly larger at 10 minutes than when freshly prepared. Interestingly, at 20 minutes, the bubble size had reduced compared to 10 minutes. However, the density of bubbles in the liquid medium was reduced, which implies that the gas trapped in larger bubbles seen at 10 minutes had evaporated from the foam phase through coalescence leaving only the smaller bubbles to the dry foam. The CNF foam stabilized with microalgae showed better stability than pulp foam as the bubbles in the CNF foam seemed to be growing only minimally with time. This finding is in agreement with the results from drainage response surface models that showed the CNF-microalgae foams exhibited smaller drainage than the pulp-microalgae foams (Fig. 2 and Fig. S2, ESI†). It should also be noted that individual pulp fibers, unlike CNF, could be seen in the foam phase, which was due to the larger dimensions of pulp fiber bundles compared to nanosized CNF.[45,46]

Green particles could be seen at the interface of the bubbles forming a darker green ring around the gas bubbles (Fig. 4 left panel). In general, the darker edges in microscopy images can be artifacts from over or under focus. However, the images in Fig. 4 right panel taken with polarization showed that there was material around the air bubbles. The material adsorbed to air bubbles was concluded to be microalgae since CNF cannot be seen with an ordinary microscope due to its nanosized dimensions. The length of CNF is typically 0.1–2 μm and the diameter 5–60 nm.[47] The effect of adsorbed microalgae was especially evident when the foam had dried and suggests that the spherical microalgae particles (Fig. 4) acted as Pickering stabilizing particles for both CNF and pulp foams. Plenty of research has been done on Pickering emulsions stabilized by various bio-materials,[15] and also some on foams generated from Pickering emulsions[48–50] with only a few works on Pickering foams.[25,51,52] Microalgae have not been previously applied as such stabilizers, however, it is likely that these microalgae particles irreversibly adsorbed onto the air–water-interface, stabilizing the bubbles long-term.[19] The microalgae used in this study had an average size of 1.9 μm and a zeta potential of −19 mV (Fig. 5A). The size distribution of the particles was quite wide, and they had a tendency to aggregate in water. The average particle size of 1.9 μm is very large compared to nanoparticles previously utilized for Pickering stabilization. Smaller particles are known to delay coalescence more efficiently than larger particles.[15] A study with starch nanoparticles as Pickering emulsion stabilizers showed that the optimal particle size was 100–220 nm and the contact angle θ_{ow} was near neutral ($\sim 90^{\circ}$) at that particle size.[25] While that study was done on emulsions, we can assume that there is some correlation to foam stabilization as well. It is thus likely that the long-term stabilizing effect in our foams came from microalgae particles rather than larger pulp fiber bundles in the pulp-microalgae foams, as was also suggested by the optimization experiments. Even though the

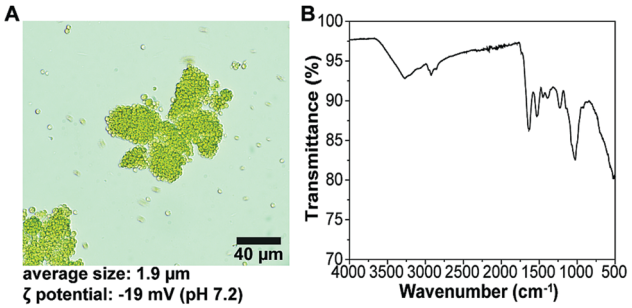

Fig. 5 (A) Light microscopy image of microalgae *C. Vulgaris* in water and the average size and surface charge of the microalgae. (B) ATR-FTIR spectrum of *C. Vulgaris*. The spectrum showed bands typical for microalgae.

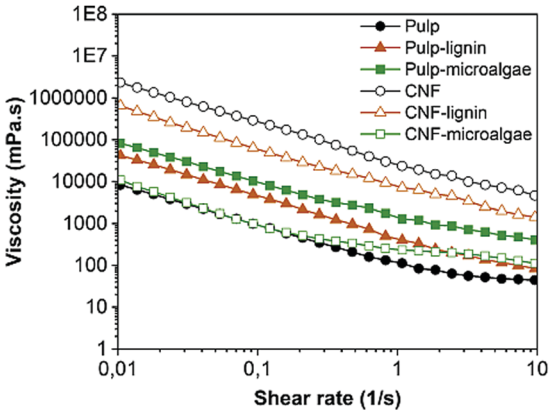

Fig. 6 The viscosity *versus* shear rate for pulp and CNF with and without lignin and microalgae. The viscosity of increased along with increasing pulp or CNF solid content.

size was not in nanoscale, the dimensions of microalgae particles were small enough compared to the bubble size of foams, allowing them to coat the bubbles.

The chemical composition of microalgae *C. vulgaris* was far more complex than any other material used in this work. The chemical structure of *C. vulgaris* was investigated using ATR-FTIR (Fig. 5B). The FTIR spectrum of *C. Vulgaris* showed a fingerprint typical for microalgae ($\nu_{NH,OH}$ 3270 cm^{-1}, ν_{CH} 2920 cm^{-1}, $\nu_{C=O}$ 1635 cm^{-1}, $\nu_{NH,CN}$ 1525 cm^{-1}, $\nu_{CH,CO}$ 1385 cm^{-1}, $\nu_P\nu_O$ 1230 cm^{-1}, ν_{C-O-C} 1030 cm^{-1}).[53,54] The composition of *C. vulgaris* can be tuned by changing the growing conditions, but it falls within the following range: 42–58% amino acids, 5–40% lipids, 12–55% carbohydrates, 1–2% pigments (chlorophyll), and minerals and vitamins.[55] The *C. vulgaris* used in this work was purchased as a dietary supplement and thus it is likely it contained a lot of amino acids and few carbohydrates. While proteins have hydrophobic and hydrophilic parts, they have no clearly defined "head and tail" and cannot by themselves reduce the surface tension of the water enough to stabilize foam.[28] However, protein-stabilized emulsions are generally more stable than those stabilized by small surfactants, due to forming of a gel-like phase around the dispersed phase, hindering coalescence.[28] It is not clear whether the algae has been broken down into its molecular constituents during the foaming process or if the cells are whole. Harvesting of *C. vulgaris* is performed by either centrifugation, filtration, flotation, or flocculation,[55,56] and the morphology of *C. vulgaris* permits high centrifugal stress without damaging its structure during the centrifugation process.[55] It is thus to be expected that the cells were intact in the material purchased for this research. The size of *C. vulgaris* cells is generally 2–10 µm, and the measured size in this work was 1.9 µm, indicating that there were whole cells present at least before generating the foam. Hence it is possible that some of the algae cells were left intact, while some others were broken down due to applied shear forces during foam generation. Algae cells have lipid layers that can adsorb onto the bubble surface creating a stabilizing layer, further enhancing the foam stability through reducing the surface tension at the gas–liquid interface.[57]

3.5 Viscosity of liquid phase

Viscosity is an important factor in the generation of foams. Usually, the viscosity influences the trapped gas content, in other words, the volume of generated foam, which in turn determines the physical properties of the foam.[41] From response surface models (Fig. 2 and 3), it was evident that increasing the cellulose and microalgae concentrations influenced both foamability and stability of the foam. The decreasing foamability and increasing stability were speculated to be due to changes in the viscosities of the liquid phase since the general understanding is that the viscosity of pulp and CNF suspensions increase along with the cellulose concentration.[58,59] Hence, the viscosity of the systems prior to introducing air and forming the foam was studied. The samples were prepared according to the volume-optimized foams (Table S1, ESI†). In principle, the viscosity of the foams increased along with pulp or CNF concentration (Fig. 6). With pulp foams, the highest viscosity was observed for pulp-microalgae (pulp concentration 12.65 g L^{-1}) foam followed by pulp-lignin (6.1 g L^{-1}) and neat pulp (7 g L^{-1}). The pulp concentration of neat pulp was slightly higher than for pulp-lignin, although the latter showed higher viscosity. This suggests that also the lignin concentration influenced the viscosity of the pulp system. With CNF, the trend was similar and CNF concentration was the major factor influencing the viscosity. Neat CNF (10.4 g L^{-1}) exhibited the highest viscosity followed by CNF-lignin (8.5 g L^{-1}) and CNF-microalgae (0.1 g L^{-1}). CNF-microalgae had significantly lower CNF concentration compared to other systems with CNF and consequently also significantly lower viscosity. However, CNF-microalgae, despite its low CNF concentration, showed almost the same viscosity as neat pulp, most likely due to the properties of the microalgae. The microalgae showed a reducing effect on the CNF foam viscosity since the sample containing the same CNF concentration as neat CNF foam (CNF g L^{-1}) and microalgae (132 g L^{-1}) had approximately 800 Pas lower viscosity than neat CNF (in ESI† Fig. S2).

3.6 Thermal conductivity

The thermal conductivity of the foams was assessed to evaluate the thermal insulation performance, which was one of the main targets for these camouflage foams. Fig. 7A shows the bulk thermal conductivity of the foams with compositions defined in

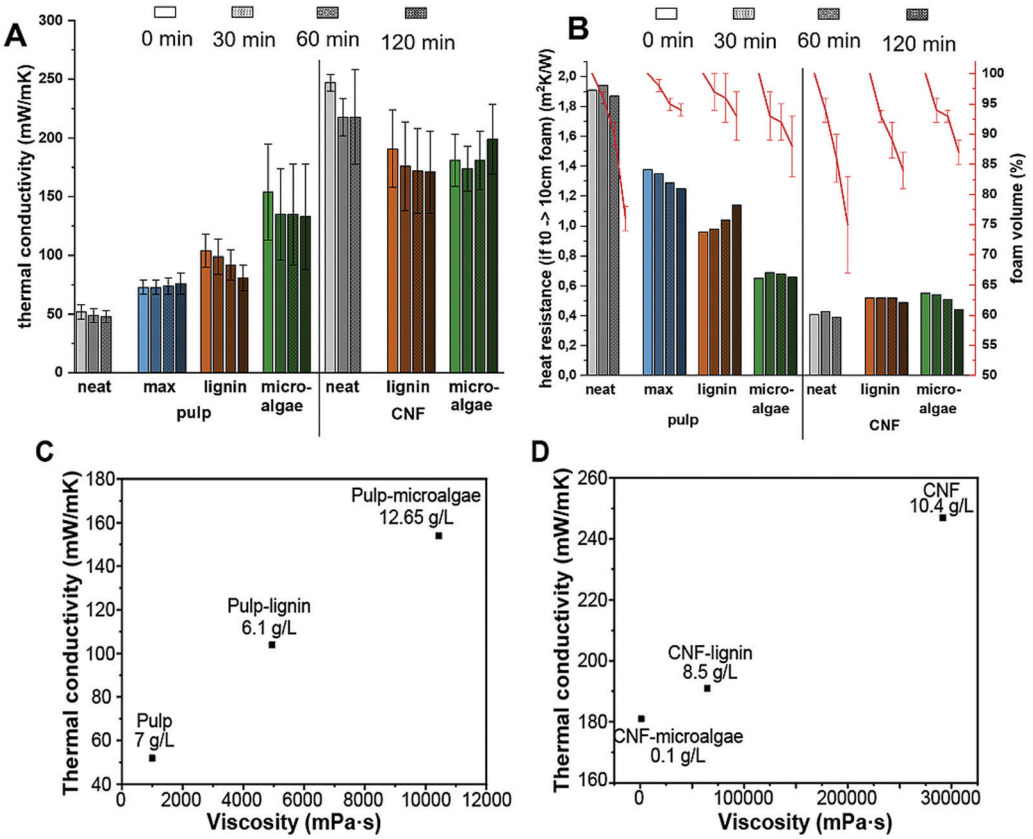

Fig. 7 (A) Thermal conductivity of the different foams. (B) Heat resistance if the initial foam thickness was assumed to be 10 cm at t = 0 min (left axis) and percentual foam volume of 270 mL (right axis). At other times than 0 minutes, the heat resistance was calculated according to percental loss of 10 cm. Neat, lignin- and microalgae pulp/CNF are the optimized foams, which compositions can be found in Table S2 (ESI†). Maximum pulp has the same SDS concentration as neat pulp and the maximum concentration of pulp, as the pulp-microalgae foam. The denser the dotted pattern, the longer the time. Conductivity for the neat samples was not measured at 120 minutes due to their substantial change in volume. The resistance of neat samples at 120 minutes is evaluated from the conductivity at 60 minutes and foam volume at 120 minutes. The relationship of thermal conductivity to viscosity for C) Pulp foams and (D) CNF foams. Viscosity was determined at a shear rate of 0.1 s^{-1}. The pulp/CNF solid content of foams is assigned in the graph. The thermal conductivity was found to be higher in foams with good stability against drainage.

Table S1 (ESI†). In addition to these foams, one additional neat pulp sample with higher solid content, referred here as maximum pulp, was prepared for the experiments. Generally, the thermal conductivity was higher for foams that had high stability in terms of low drainage due to high cellulose content. The smaller the drainage, the more water retained in the foam phase. Since water has higher thermal conductivity than air, the thermal insulation was found to be poorer in the more stable foams. The maximum pulp had a higher pulp concentration than neat pulp, 12.65 g L^{-1} *versus* 7 g L^{-1}, and consequently had better drainage stability (Fig. 2) and more water retained in the foam phase. Thus, the maximum pulp sample exhibited higher thermal conductivity than the neat pulp sample. A similar relationship of good stability and high thermal conductivity was also observed for the other foams. The stability of the pulp-microalgae foam was increased thanks to the microalgae content (Fig. 2), and thus the higher water content led to even higher thermal conductivity. The addition of lignin to some extent increased the conductivity, however, pulp-microalgae showed higher stability and thermal conductivity than pulp-lignin foam containing 6.1 g L^{-1} of cellulose. The stabilizing effect of microalgae and lignin was evident since the foams without them collapsed faster, and measuring their thermal conductivity at 120 min was impossible.

The CNF foams in general had higher thermal conductivity compared to pulp foams. Even though the cellulose content of CNF-microalgae foam was extremely low compared to pulp foams, its thermal conductivity was around 18% higher than the highest thermal conductivity for pulp foams. The higher thermal conductivity of CNF foams was considered to be due to its hygroscopic nature and fine fibril network that allows it to gel at low concentrations. Neat CNF (10.4 g L^{-1}) had a higher CNF concentration than CNF-lignin (8.5 g L^{-1}), which led to higher conductivity. The dry nanocellulose foams and aerogels have been shown to display thermal conductivities from 20 to 40 mW m^{-1} K^{-1}.[60–62] Herein, only the neat pulp foam (~50 mW m^{-1} K^{-1}) reached close to those values. But as the foams presented here were measured as wet, the comparison to dry foams and aerogels is not straightforward. The dry nanocellulose-based foams with excellent thermal conductivities however exhibit an increase in thermal conductivity, too, if the relative humidity is elevated up to 80%.[61] Commonly used current insulating materials exhibit

thermal conductivity values as follows: expanded or extruded polystyrene (30–44 mW m^{-1} K^{-1}), mineral wood (30–40 mW m^{-1} K^{-1}), and cork (40–50 mW m^{-1} K^{-1}).[63] Many of the samples presented here are relatively far from these values but they are all dry materials. Removing some water, *e.g.* by drying, could thus help the insulating properties.

Heat resistance describes the foam's ability to resist the heat transfer and takes the foam thickness into account. Thus, it shows the stability of insulation properties better than conductivity when foams degrade. Neat and maximum pulp samples showed high heat resistance values at first but their resistance decreased after 60 minutes. On the other hand, lignin and micro-algae samples showed lower resistance but no loss in resistance during 120 minutes. All pulp foams had higher heat resistance than the CNF foams. The values for all CNF foams were similar and quite close to pulp-microalgae.

From the application point of view, materials with lower thermal conductivity and higher heat resistance are better insulators than more conductive and less heat resistant materials. This favors using pulp over CNF, in addition to economic aspects. Microalgae seemed to decrease the heat resistance, which hampers the insulating properties. There is plenty of literature on dry foams, but to the best of our knowledge, the conductivity of wet foams has not been measured before. As the foams were measured wet, structural changes occurred during the tests. This caused a quite large deviation in conductivity and volume for some of the foams (see standard deviation bars in Fig. 7A and B).

3.7 Reflectance spectra

The reflectance spectrum is of utmost importance for camouflage materials. The optical camouflage performance of the foams was investigated by evaluating the average reflectance spectra of the pulp foams compared to natural reference materials from the boreal forest. The thermal conductivity of pulp foams was found to be lower than CNF, and since the pulp is economically more feasible for large-scale foam production, pulp foams were selected for the application. The reflectance spectra across visible to near-infrared light ranges (400–1000 nm) were determined from freshly generated foams and aged foams after 7 days (Fig. 8). As seen in the figure, the reflectance of the neat pulp foam decreased substantially over time in all wavelengths during the 7 day follow-up period, whereas reflectance spectra of lignin and microalgae containing foams changed only subtly (in ESI† Fig. S3). This can be attributed to the neat pulp foam turning transparent during foam aging, whereas the lignin and microalgae foams retained their pigments even though the foam structure was lost. The colorant absorption can be observed from the visible region (400–700 nm) region. It can be observed that the reflectance of the microalgae foam decreased over time. The chlorophyll a and b pigments giving the green color for microalgae have a characteristic absorption band around 550 nm, which was found also from the foam samples.[64] The observed decrease and shift in reflectance suggest that the structures of the chlorophylls change with time. Chlorophylls are sensitive compounds, and they degrade easily due to air, heat, and light.[65] The reflectance spectra of lignin foam altered less than the spectra of microalgae foam, although some small alterations took place as the reflectance slightly increased over 7 days.

The reflectance spectral characteristics of the colored foams were compared to natural green and brown reference materials. Lignin foams had the closest spectral fingerprint to the natural reference materials. The slope of the brown curve is similar to published requirements for the L boreal woodland camouflage materials.[64] With microalgae, the differences in visible light wavelengths were quite large compared to reference materials, most likely due to the different pigment compositions of samples. In green photosynthetic biomasses, chlorophylls are often present with other pigments, such as carotenoids and anthocyanins, which influence the overall absorption and color properties.[66,67] Birch bark and aged neat pulp foam showed relatively similar spectral properties. However, all foams exhibited a distinctive drop in reflectance at 950 nm, which was not present in the spectra of any natural materials. This band at 950–970 nm is attributed to water absorption.[68] It suggests that the foam samples had higher water content than the natural reference materials. This indicates that the visible light spectral performance of the foams is satisfactory to camouflage targets to the forest environment. However, the presence of this distinctive reflectance band due to the water content reveals the camouflage foam when imaged with a hyper- or multispectral camera. However, continuing the research to develop dry foams from

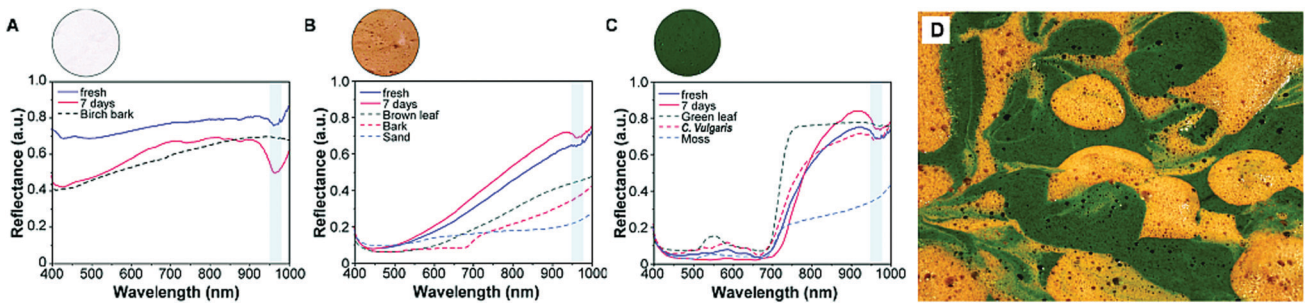

Fig. 8 Average reflectance spectra of (A) bleached pulp as fresh and after 7 days, (B) lignin stabilized pulp foam as fresh and after 7 days, and (C) microalgae stabilized pulp foam as fresh and after 7 days. The natural reference materials are marked with dotted lines to correspondingly colored foam. All foams showed a band around 950 nm, which can be attributed to the presence of water. (D) Photograph of patterned foam.

these substances could both increase insulation properties and enhance the reflectance spectral characteristics.

In this work, only one green and brown shade were used and in nature there are a plethora of shades. The green and brown foam were mixed together, however, the resulting foam was mostly predominantly green and the hysperspectra resembled the spectra of the green foam. A better strategy to obtain a realistic camouflage foam was patterning the two colors (Fig. 8D). In forests there are few solid-colored surfaces, so engineering a suitable camouflage pattern using the colored foams would be needed for these foams to work in camouflage applications.

4. Conclusions

In this work, cellulosic wet foams from surfactant, bleached pulp or cellulose nanofibrils (CNF), and microalgae or kraft lignin were prepared for creating lightweight material for camouflage application to be used in a boreal forest environment. Increasing the solid content of pulp or CNF improved the stability of wet foams, but microalgae and lignin stabilized the foams even further. On the other hand, increasing the pulp and CNF solids content simultaneously decreased the foamability of the system. In addition to cellulose solid content, the stabilizing lignin and microalgae reduced the foam yield as well and the influence of microalgae was more significant than lignin. The camouflage properties of wet foams were investigated in terms of thermal conductivity and spectral properties. The thermal insulation performance varied depending on the stability and water content of the foam but even thermal conductivity comparable to dry nanocellulose-based foam was observed. The visual appearance of the foams was found to be similar to natural reference materials from the boreal forest. However, the water content of the foams made them distinguishable from natural references in the near-infrared (NIR) region. To improve the NIR spectral range camouflage properties further, decreasing the water content of foams could be considered. Overall, this work demonstrated that wet cellulose-based foams stabilized using microalgae and lignin are fast and scalable renewable materials applicable for camouflage. Due to the strong dependence between foam stability and camouflage performance, some compromises are needed while designing the optimal foam system for the application.

Conflicts of interest

The authors declare that they have no conflict of interest.

Acknowledgements

The authors thank Dr Muhammad Farooq for assisting with the Olympus BX53M microscope, Marja Kärkkäinen for providing the bleached pulp, and Tuyen Nguyen for providing cellulose nanofibrils. This work was funded by The Scientific Advisory Board for Defense (MATINE, 2500M-0110). We are grateful for the support by the FinnCERES Materials Bioeconomy Ecosystem, and this work made use of Aalto University Bioeconomy Infrastructure. Work was also supported by The Academy of Finland project "Bio Based Dyes and Pigments for Colour Palette (Bio-Colour)" (Grant 327209).

References

1 M. Stevens and S. Merilaita, Animal camouflage: Current issues and new perspectives, *Philos. Trans. R. Soc., B*, 2009, **364**, 423–427.
2 O. N. Laschuk, I. Ebralidze, E. Bradley Easton and V. O. Zenkina, Post-Synthetic Color Tuning of the Ultra-Effective and Highly Stable Surface-Confined Electrochromic Monolayer: Shades of Green for Camouflage Materials, *ACS Appl. Mater. Interfaces*, 2021, **13**(33), 39573–39583.
3 H. Yu, S. Shao, L. Yan, H. Meng, Y. He, C. Yao, P. Xu, X. Zhang and W. Huang, Side-chain engineering of green color electrochromic polymer materials: toward adaptive camouflage application, *J. Mater. Chem. C*, 2016, **4**, 2269–2273.
4 D. Liu, X. Shouhu, Y. Qiao, Z. Meng, P. Wang and D. Yan, Research Progress of Bionic Adaptive Camouflage Materials, *Front. Mater.*, 2021, **8**, 637664.
5 K. Fortuniak, G. Redlich, E. Obersztyn, M. Olejnik, A. Bartczak and I. Król, Assessment and verification of the functionality of new, multi-component, camouflage materials, *Fibres Text. East. Eur.*, 2013, **101**(5), 73–79.
6 A. D. Roberts, W. Finnigan, E. Wolde-Michael, P. Kelly, J. J. Blaker and S. Hay, *et al.*, Synthetic Biology Prospective Synthetic biology for fibers, adhesives, and active camouflage materials in protection and aerospace, *MRS Commun.*, 2019, **9**(2), 486–504.
7 M. J. Khan, H. S. Khan, A. Yousaf, K. Khurshid and A. Abbas, Modern Trends in Hyperspectral Image Analysis: A Review, *IEEE Access*, 2018, **6**, 14118–14129.
8 A. Demharter, Polyurethane rigid foam, a proven thermal insulating material for applications between +130 °C and −196 °C, *Cryogenics*, 1998, **38**(1), 113–117.
9 M. Modesti, A. Lorenzetti and S. Besco, Influence of Nanofillers on Thermal Insulating Properties of Polyurethane Nanocomposites Foams, *Polym. Eng. Sci.*, 2007, **47**(9), 1351–1358.
10 P. Wang, N. Aliheidari, X. Zhang and A. Ameli, Strong ultralight foams based on nanocrystalline cellulose for high-performance insulation, *Carbohydr. Polym.*, 2019, **218**, 103–111.
11 S. Ahmadzadeh, A. Nasirpour, J. Keramat, N. Hamdami, T. Behzad and S. Desobry, Nanoporous cellulose nanocomposite foams as high insulated food packaging materials, *Colloids Surf., A*, 2015, **468**, 201–210.
12 A. A. Septevani, D. A. C. Evans, P. K. Annamalai and D. J. Martin, The use of cellulose nanocrystals to enhance the thermal insulation properties and sustainability of rigid polyurethane foam, *Ind. Crops Prod.*, 2017, **107**, 114–121.
13 W. Leng and B. Pan, Thermal Insulating and Mechanical Properties of Cellulose Nanofibrils Modified Polyurethane

Foam Composite as Structural Insulated Material, *Forests*, 2019, **10**(2), 200.

14 Z. Cai, Y. Li, H. He, Q. Zeng, J. Long and L. Wang, *et al.*, Catalytic Depolymerization of Organosolv Lignin in a Novel Water/Oil Emulsion Reactor: Lignin as the Self-Surfactant, *Ind. Eng. Chem. Res.*, 2015, **54**(46), 11501–11510.

15 S. Lam, K. P. Velikov and O. D. Velev, Pickering stabilization of foams and emulsions with particles of biological origin, *Current Opinion in Colloid and Interface Science*, Elsevier Ltd, 2014, vol. 19, pp. 490–500.

16 J. Viitala, T. Lappalainen and M. Järvinen, Sodium dodecyl sulphate (SDS) residue analysis of foam-formed cellulose-based products, *Nord. Pulp Pap. Res. J.*, 2020, **35**(2), 261–271.

17 R. Li, J. Du, Y. Zheng, Y. Wen, X. Zhang and W. Yang, *et al.*, Ultra-lightweight cellulose foam material: preparation and properties, *Cellulose*, 2017, **24**(3), 1417–1426.

18 N. Lavoine and L. Bergström, Nanocellulose-based foams and aerogels: Processing, properties, and applications, *J. Mater. Chem. A*, 2017, **5**(31), 16105–16117.

19 T. J. Muth and A. J. Lewis, Microstructure and Elastic Properties of Colloidal Gel Foams, *Langmuir*, 2017, **33**(27), 6869–6877.

20 N. T. Cervin, E. Johansson, J.-W. Benjamins and L. Wågberg, Mechanisms Behind the Stabilizing Action of Cellulose Nanofibrils in Wet-Stable Cellulose Foams, *Biomacromolecules*, 2015, **16**(3), 822–831.

21 W. Xiang, Interfacial Stabilization of Multiphase Systems with (Ligno)cellulosic (Nano)materials and Surfactants, [dissertation]. Espoo (FIN) Aalto University, 2019.

22 S. U. Org, Transforming Our World: The 2030 Agenda For Sustainable Development United Nations United Nations Transforming Our World: The 2030 Agenda For Sustainable Development.

23 Z. Hu, R. Xu, E. D. Cranston and R. H. Pelton, Stable Aqueous Foams from Cellulose Nanocrystals and Methyl Cellulose, *Biomacromolecules*, 2016, **17**(12), 4095–4099.

24 S. S. Borkotoky, G. Chakraborty and V. Katiyar, Thermal degradation behaviour and crystallization kinetics of poly (lactic acid) and cellulose nanocrystals (CNC) based microcellular composite foams, *Int. J. Biol. Macromol.*, 2018, **118**, 1518–1531.

25 S. Ge, L. Xiong, M. Li, J. Liu, J. Yang and R. Chang, *et al.*, Characterizations of Pickering emulsions stabilized by starch nanoparticles: Influence of starch variety and particle size, *Food Chem.*, 2017, **234**, 339–347.

26 N. Yildirim, S. M. Shaler, D. J. Gardner, R. Rice and D. W. Bousfield, Cellulose nanofibril (CNF) reinforced starch insulating foams. *Cellulose*. 2014, [cited 2021 Mar 4], 21(6), 4337–4347, https://link.springer.com/article/10.1007/s10570-014-0450-9.

27 L. Indrawati and G. Narsimhan, Characterization of protein stabilized foam formed in a continuous shear mixing apparatus, *J. Food Eng.*, 2008, **88**(4), 456–465.

28 S. Damodaran, Protein Stabilization of Emulsions and Foams, *J. Food Sci.*, 2005, **70**(3), R54–R66.

29 V. Mimini, V. Kabrelian, K. Fackler, H. Hettegger, A. Potthast and T. Rosenau, Lignin-based foams as insulation materials: A review, *Holzforschung*, 2019, **73**(1), 117–130.

30 G. Tondi, M. Link, C. Kolbitsch, J. Gavino, P. Luckeneder and A. Petutschnigg, *et al.*, Lignin-based foams: Production process and characterization, *BioResources*, 2016, **11**(2), 2972–2986.

31 M. Shahid, Shahid-Ul-Islam and F. Mohammad, Recent advancements in natural dye applications: A review, *J. Cleaner Prod.*, 2013, **53**, 310–331.

32 S. Li, J. A. Willoughby and O. J. Rojas, Oil-in-Water Emulsions Stabilized by Carboxymethylated Lignins: Properties and Energy Prospects, *ChemSusChem*, 2016, **9**(17), 2460.

33 G. A. Blackburn, Hyperspectral remote sensing of plant pigments, *J. Exp. Bot.*, 2007, **58**(4), 855–867.

34 H. Peltola, K. Immonen, L.-S. Johansson, J. Virkajärvi and D. Sandquist, *Influence of pulp bleaching and compatibilizer selection on performance of pulp fiber reinforced PLA biocomposites*, 2019.

35 A. Swerin, L. Odberg and T. Lindström, Deswelling of hardwood kraft pulp fibers by cationic polymers, *Nord. Pulp Pap. Res. J.*, 1990, **5**(4), 188–196.

36 M. Farooq, T. Zou, G. Riviere, M. H. Sipponen and M. Österberg, Strong, Ductile, and Waterproof Cellulose Nanofibril Composite Films with Colloidal Lignin Particles, *Biomacromolecules*, 2019, **20**(2), 693–704.

37 M. Österberg, J. Vartiainen, J. Lucenius, U. Hippi, J. Seppälä and R. Serimaa, *et al.*, A Fast Method to Produce Strong NFC Films as a Platform for Barrier and Functional Materials, *ACS Appl. Mater. Interfaces*, 2013, **5**(11), 4640–4647.

38 P. Eronen, J. Laine, J. Ruokolainen and M. Österberg, Comparison of Multilayer Formation Between Different Cellulose Nanofibrils and Cationic Polymers, *J. Colloid Interface Sci.*, 2012, **373**(1), 84–93.

39 T. Lohtander, R. Herrala, P. Laaksonen, S. Franssila and M. Österberg, Lightweight lignocellulosic foams for thermal insulation, *Cellulose*, 2022, DOI: 10.1007/s10570-021-04385-6.

40 D. Klemm, F. Kramer, S. Moritz, T. Lindström, M. Ankerfors and D. Gray, *et al.*, Nanocelluloses: A new family of nature-based materials, *Angew. Chem., Int. Ed.*, 2011, **50**, 5438–5466.

41 W. Drenckhan and A. Saint-Jalmes, The science of foaming, *Advances in Colloid and Interface Science*, Elsevier B. V., 2015, vol. 222, pp. 228–59.

42 J. C. Sara, C. Thad, M. Tapio, L. Tuomas Hänninen, J. Cucharero and Á. T. Lokki, *et al.*, Sound absorption properties of wood-based pulp fibre foams, *Cellulose*, 2021, **28**, 4267–4279.

43 S. He, C. Liu, X. Chi, Y. Zhang, G. Yu and H. Wang, *et al.*, Bio-inspired lightweight pulp foams with improved mechanical property and flame retardancy via borate cross-linking, *Chem. Eng. J.*, 2019, **371**, 34–42.

44 W. Drenckhan and S. Hutzler, Structure and energy of liquid foams, *Adv. Colloid Interface Sci.*, 2015, **224**, 1–16.

45 D. Klemm, B. Heublein, H. P. Fink and A. Bohn, Cellulose: Fascinating biopolymer and sustainable raw material, *Angew. Chem., Int. Ed.*, 2005, **44**, 3358–3393.

46 D. Klemm, F. Kramer, S. Moritz, T. Lindström, M. Ankerfors and D. Gray, *et al.*, Nanocelluloses: A New Family of Nature-Based Materials, *Angew. Chem., Int. Ed.*, 2011, **50**(24), 5438–5466.

47 D. Klemm, E. D. Cranston, D. Fischer, M. Gama, S. A. Kedzior and D. Kralisch, *et al.*, Nanocellulose as a natural source for groundbreaking applications in materials science: Today's state, *Mater. Today*, 2018, **21**(7), 720–748.

48 J. B. Mougel, P. Bertoncini, B. Cathala, O. Chauvet and I. Capron, Macroporous hybrid Pickering foams based on carbon nanotubes and cellulose nanocrystals, *J. Colloid Interface Sci.*, 2019, **544**, 78–87.

49 H. M. Ahsan, Y. Pei, X. Luo, Y. Wang, Y. Li and B. Li, *et al.*, Novel stable pickering emulsion based solid foams efficiently stabilized by microcrystalline cellulose/chitosan complex particles, *Food Hydrocolloids*, 2020, **108**, 106044.

50 X. Zhang, J. Zhou, J. Chen, B. Li, Y. Li and S. Liu, Edible foam based on pickering effect of bacterial cellulose nanofibrils and soy protein isolates featuring interfacial network stabilization, *Food Hydrocolloids*, 2020, **100**, 105440.

51 P. Ravi Anusuyadevi, V. A. Riazanova, S. M. Hedenqvist and J. A. Svagan, Floating Photocatalysts for Effluent Refinement Based on Stable Pickering Cellulose Foams and Graphitic Carbon Nitride (g-C3N4), *ACS Omega*, 2020, **5**(35), 22411–22419.

52 X. Li, B. S. Murray, Y. Yang and A. Sarkar, Egg white protein microgels as aqueous Pickering foam stabilizers: Bubble stability and interfacial properties, *Food Hydrocolloids*, 2020, **98**, 105292.

53 N. Kahzad and A. Salehzadeh, Green Synthesis of $CuFe_2O_4$@Ag Nanocomposite Using the Chlorella vulgaris and Evaluation of its Effect on the Expression of norA Efflux Pump Gene Among Staphylococcus aureus Strains, *Biol. Trace Elem. Res.*, 2020, **198**(1), 359–370.

54 M. Kumar, A. K. Singh and M. Sikandar, Study of sorption and desorption of Cd(II) from aqueous solution using isolated green algae Chlorella vulgaris, *Appl. Water Sci.*, 2018, **8**(8), 1–11.

55 C. Safi, B. Zebib, O. Merah, P. Y. Pontalier and C. Vaca-Garcia, Morphology, composition, production, processing and applications of Chlorella vulgaris: A review, *Renewable Sustainable Energy Rev.*, 2014, **35**, 265–278.

56 E. Molina Grima, E. H. Belarbi, F. G. Acién Fernández, A. Robles Medina and Y. Chisti, Recovery of microalgal biomass and metabolites: process options and economics, *Biotechnol. Adv.*, 2003, **20**(7–8), 491–515.

57 U. T. Gonzenbach, A. R. Studart, E. Tervoort and L. J. Gauckler, Ultrastable Particle-Stabilized Foams, *Angew. Chem., Int. Ed.*, 2006, **45**(21), 3526–3530.

58 L. Mendoza, W. Batchelor, R. F. Tabor and G. Garnier, Gelation mechanism of cellulose nanofibre gels: A colloids and interfacial perspective, *J. Colloid Interface Sci.*, 2018, **509**, 39–46.

59 E. Lasseuguette, D. Roux and Y. Nishiyama, Rheological properties of microfibrillar suspension of TEMPO-oxidized pulp, *Cellul*, 2007, **153**(3), 425–433.

60 K. Sakai, Y. Kobayashi, T. Saito and A. Isogai, Partitioned airs at microscale and nanoscale: Thermal diffusivity in ultrahigh porosity solids of nanocellulose, *Sci. Rep.*, 2016, **6**(1), 1–7.

61 K. Apostolopoulou-Kalkavoura, N. Gordeyeva, L. Lavoine and V. Bergström, Thermal conductivity of hygroscopic foams based on cellulose nanofibrils and a nonionic polyoxamer, *Cellulose*, 2018, **25**(2), 1117–1126.

62 Y. Kobayashi, T. Saito and A. Isogai, Aerogels with 3D Ordered Nanofiber Skeletons of Liquid-Crystalline Nanocellulose Derivatives as Tough and Transparent Insulators, *Angew. Chem., Int. Ed.*, 2014, **53**(39), 10394–10397.

63 E. Cuce, P. M. Cuce, C. J. Wood and S. B. Riffat, Toward aerogel based thermal superinsulation in buildings: A comprehensive review, *Renewable Sustainable Energy Rev.*, 2014, **34**, 273–299.

64 V. Rubežiene, I. Padleckiene, J. Baltušnikaite and S. Varnaite, Evaluation of camouflage effectiveness of printed fabrics in visible and near infrared radiation spectral ranges, *Medziagotyra*, 2008, **14**(4), 361–365.

65 P. Matile, S. Hörtensteiner and H. Thomas, Chlorophyll Degradation, *Annu. Rev. Plant Physiol. Plant Mol. Biol.*, 1999, **50**, 67–95.

66 K. Kitada, S. Machmudah, M. Sasaki, M. Goto, Y. Nakashima and S. Kumamoto, *et al.*, Supercritical CO2 extraction of pigment components with pharmaceutical importance from Chlorella vulgaris, *J. Chem. Technol. Biotechnol.*, 2009, **84**(5), 657–661.

67 A. A. Gitelson, G. P. Keydan and M. N. Merzlyak, Three-band model for noninvasive estimation of chlorophyll, carotenoids, and anthocyanin contents in higher plant leaves, *Geophys. Res. Lett.*, 2006, **33**(11), L11402.

68 J. Peñuelas, I. Filella, C. Biel, L. Serrano and R. Savé, The reflectance at the 950–970 nm region as an indicator of plant water status, *Int. J. Remote Sens.*, 1993, **14**(10), 1887–1905.